Photodiagnosis and Photodynamic Therapy 45 (2024) 103952

Contents lists available at ScienceDirect

Photodiagnosis and Photodynamic Therapy

journal homepage: www.elsevier.com/locate/pdpdt

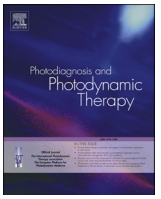

Photodynamic inactivation of methicillin-resistant *Staphylococcus aureus* by using Giemsa dye as a photosensitizer

Cynthia S.A. Caires [a,b], Alessandra R. Lima [a,c], Thalita H.N. Lima [a,c], Cicera M. Silva [a], Leandro O. Araujo [a], Laís F. Aguilera [a], Valter A. Nascimento [d], Anderson R.L. Caires [a,*], Samuel L. Oliveira [a,*]

[a] *Instituto de Física, Universidade Federal de Mato Grosso do Sul, 79070-900, Campo Grande, MS CP 549, Brazil*
[b] *Escola de Saúde, Santa Casa de Campo Grande, Campo Grande, MS 79002-201, Brazil*
[c] *Instituto de Física de São Carlos, Universidade de São Paulo, 13560-970, São Carlos, SP CP 369, Brazil*
[d] *Faculdade de Medicina, Universidade Federal de Mato Grosso do Sul, 79070-900, Campo Grande, MS CP 549, Brazil*

ARTICLE INFO

Keywords:
Multidrug-resistant bacteria
Methicillin-resistant Staphylococcus aureus
Giemsa
Antimicrobial photodynamic inactivation
Photodynamic Therapy

ABSTRACT

The rise of antibiotic-resistant bacteria calls for innovative approaches to combat multidrug-resistant strains. Here, the potential of the standard histological stain, Giemsa, to act as a photosensitizer (PS) for antimicrobial photodynamic inactivation (aPDI) against methicillin-sensitive *Staphylococcus aureus* (MSSA) and methicillin-resistant *Staphylococcus aureus* (MRSA) strains is reported. Bioassays were performed using various Giemsa concentrations (ranging from 0.0 to 20.0 μM) under 625 nm illumination at a light dose of 30 J cm^{-2}. Remarkably, Giemsa completely inhibited the growth of MSSA and MRSA bacterial colonies for concentrations at 10 μM and higher but exhibited no inhibitory effect without light exposure. Partition coefficient analysis revealed Giemsa's affinity for membranes. Furthermore, we quantified the production of reactive oxygen species (ROS) and singlet oxygen ($^1O_2$) to elucidate the aPDI mechanisms underlying bacterial inactivation mediated by Giemsa. These findings highlight Giemsa stain's potential as a PS in aPDI for targeting multidrug-resistant bacteria.

1. Introduction

The emergence of the Wright-Giemsa stain is linked to the discovery of the etiological agent of malaria (Plasmodium) by Frenchman Alphonse Laveran in 1880 using methylene blue [1–3]. However, accurate malaria diagnosis was still tricky in the early 20th century due to the staining method and reproducibility [2]. In 1904, Gustav Giemsa prepared a dye called azure I, a hybrid mixture of azure A and azure B, with traces of azure C and methylene violet [3]. After obtaining Azure I, Giemsa formed a more definitive and stable compound combining Azure I with eosin [4]. The Giemsa stain was designed primarily to identify malaria parasites because of the high-quality staining of the nuclear membrane. Additionally, the Giemsa staining method was adapted for histology to display chromatin, and the nuclear membrane remains one of the staining techniques most used in biomedical laboratories worldwide [4,5]

Most recently, some studies demonstrated that Giemsa stain can be applied as a photo-responsive agent, acting as a photosensitizer in the photodynamic inactivation of microorganisms and insect vectors [6–8]. Caires et al. demonstrated that Giemsa stain photoinactivates Gram-positive and Gram-negative bacteria under red light illumination [6,7] as well as eliminates larvae of *Aedes aegypti* when subjected to white-light radiation from RGB LEDs or sunlight [8]. In this context, Giemsa stain emerges as a promising candidate to be used in antimicrobial photodynamic inactivation (aPDI) because it is less cytotoxic on normal mammalian cells and is more effective when compared to methylene blue and toluidine blue, two photosensitizers commonly used in aPDI, demanding low concentrations and light doses to efficiently photoinactivate bacteria [6].

Staphylococcus aureus is a common commensal bacterium in our lives; it is in the human microbiome and can potentially induce a variety of infections targeting specific organs, with the skin and subcutaneous tissues being the most frequently affected. It can also lead to more severe invasive infections, such as osteomyelitis, meningitis, pneumonia, lung abscess, and empyema [9,10]. Infections caused by *S. aureus* are a problem mainly in hospital environments, leading to surgical

* Corresponding authors.
E-mail addresses: anderson.caires@ufms.br (A.R.L. Caires), samuel.oliveira@ufms.br (S.L. Oliveira).

https://doi.org/10.1016/j.pdpdt.2023.103952
Received 8 September 2023; Received in revised form 9 December 2023; Accepted 22 December 2023
Available online 24 December 2023

complications and respiratory and blood infections [11,12]. Presently, methicillin-resistant *Staphylococcus aureus* (MRSA) infections are a global public health challenge, as they are associated with higher mortality rates compared to those caused by methicillin-sensitive *Staphylococcus aureus* (MSSA) strains [13]. Due to the virulence characteristics of this pathogen, the emergence of resistant strains is a reason for concern worldwide. In 1960, an MRSA strain was reported, just one year after methicillin had been used as an antibiotic [14,15]. Studies estimate that individuals infected with MRSA have a 64 % higher risk of mortality than those infected with MSSA [16]. MRSA has become the leading cause of healthcare-associated infections in Europe, with over 171,000 nosocomial MRSA infections annually [17]. In the United States, MRSA accounts for a minimum of 80,000 infections yearly, resulting in approximately 11,000 deaths [18]. In light of this, it has been considered the major threat among antibiotic-resistant agents of morbidity and mortality by the Centers for Disease Control and Prevention (CDC) [19,20]. The World Health Organization (WHO) has identified antimicrobial-resistant microorganisms (AMR) as one of the top ten global public health threats [12,21]. AMR was associated with approximately 4.95 million deaths worldwide in 2019 [22,23]. According to a report by O'Neill (2016), if no action is taken, there will be a staggering 10 million deaths annually by 2050 due to AMR-related infections. Besides, the AMR impacts would also result in an annual global gross domestic product reduction of around $2 trillion by 2050 [24,25]. Therefore, the rise of antibiotic-resistant bacteria has presented a significant healthcare challenge, necessitating new strategies to combat these pathogens effectively. Conventional antibiotic treatments often face the problem of resistance [26], underscoring the importance of exploring alternative approaches.

In this context, aPDI has emerged as a promising method to inactivate multidrug-resistant bacteria by oxidative damaging bacterial cells using light-absorbers (photosensitizers) to generate reactive oxygen species (ROS) and singlet oxygen ($^1O_2$) through change transfer and energy transfer, respectively [27–30]. Here, it is reported the efficacy of Giemsa stain as a photosensitizer (PS) to photoinactivate MRSA and MSSA under 625 nm illumination and the aPDI mechanisms responsible for bacterial inactivation promoted by Giemsa.

2. Materials and methods

2.1. Photosensitizer

The Giemsa stain (Eosin methylene blue, EMB, Sigma Vetec®, Brazil) was tested as a PS in the aPDI experiments.

2.2. Photoinactivation assay

2.2.1. Bacterial strains and culture conditions

An MSSA strain (ATCC 25923, Bioscan, Itu, Brazil) and a clinically isolated MRSA strain (GenBank accession number Mh087437, HU, Campo Grande, Brazil) were used. They were maintained at −70 °C in Brain Heart Infusion Broth (BHI) (KASVI, São José dos Pinhais, PR, Brazil) containing glycerol 20 % vv^{-1}. The bacterial suspensions were prepared with 40 μL of the bacterial strain added to 4 mL of BHI and incubated for 24 h at 37 °C. The bacterial inoculum at 1.5×10^8 CFU mL^{-1} was prepared for the aPDI experiments in physiological saline (0.9 % NaCl, Sorimax, Campo Grande, Brazil).

2.2.2. aPDI Assay

The Giemsa concentrations were 0.0 (negative control), 1.0, 2.5, 5.0, 10.0, and 20.0 μM diluted in 2 mL of a saline solution containing the bacterial inoculum at 1.5×10^8 CFU mL^{-1}. Then, the samples were incubated at 120 rpm for 30 min at 37 °C. After incubation, bacterial suspensions were placed in 96-well plates (200 μL per well) and separated into two experimental groups: (i) samples placed in the dark and (ii) samples subjected to red light illumination at 625 nm with a light dose of 30 J cm^{-2} using a homemade light-emitting diodes device [7]. Finally, for both irradiated and not-irradiated samples, a serial dilution was performed until 1:32. The total bacteria number was determined by the spread plate method using the plate count agar (PCA; Neogen Corp., Michigan, USA) medium and the colony-forming units (CFU) were counted 18 h after incubation at 37 °C. All experiments were carried out in triplicate.

2.2.3. Statistical analysis

Quantitative and statistical analyses were done using the OriginLab software, considering the triplicates, PS concentrations, and light exposure conditions (illuminated and non-illuminated). The CFU mL^{-1} values were converted into $\log_{10}$ and submitted to analysis of variance and comparisons of the means using Student's *t*-test with a confidence level of 95 % ($p < 0.05$) for paired samples.

2.2.4. Morphological evaluation of bacteria by scanning electron microscopy

The bacteria morphology was examined with a scanning electron microscope (SEM, JEOL model JSM-6380LV). The investigations encompassed irradiated and non-irradiated bacteria subjected to Giemsa stain and control samples (bacteria in distilled water). The experiments were done with approximately 200 μL of each sample placed into an Eppendorf containing 200 μL of phosphate buffer solution (PBS) at pH 7.0 immediately after completing the aPDI assay. The samples underwent multiple centrifugation cycles at 3000 rpm for 5 min, always discarding the supernatant each time. The centrifugations were conducted in the following sequence: PBS (three times), 70, 80, 90 % ethanol, and absolute ethanol. The resulting precipitate was dispersed in absolute ethanol and stored in the refrigerator. Glass coverslips (1 × 1 cm) were cut and cleaned in an ultrasonic sonicator using water/soup, ethanol, and acetone for 20 min. The glass substrates were coated with glutaraldehyde and dried overnight under ambient conditions to fix the bacteria. After deposition onto the glass surface, the samples were coated with a thin layer of gold using a sputter coater and attached to the SEM sample holders using conductive carbon tape. Images were captured under the following conditions: 15 kV, spot size 10, and a working distance of 8 mm.

2.3. Photophysical and photochemical characterization

1,3-diphenylisobenzofuran (DPBF) and dihydroethidium (DHE) were acquired from Sigma-Aldrich (São Paulo, Brazil) to probe the capability of Giemsa stain to produce reactive oxygen species (ROS) and singlet oxygen ($^1O_2$) through the charge transfer (type I) and energy transfer (type II) photochemical pathways, respectively.

2.3.1. Singlet Oxygen ($^1O_2$) generation

The quantum yield of singlet oxygen generation ($\varnothing_\Delta$) for Giemsa was determined using methylene blue (Vetec®, Brazil) as the standard PS and DPBF as the $^1O_2$ probe [31,32]. The DPBF was dissolved in dimethyl sulfoxide (DMSO) to 1 mM. Giemsa and methylene blue (MB) standard solution were prepared in DMSO at a concentration of 30 μM. Measurements were performed with 2000 μL of DMSO, 400 μL of Giemsa (sample) or MB (standard), and 200 μL of DPBF solution at 1 mM in a four-sided polished quartz cuvette with optical path of 10 mm. The final concentration of photosensitizer (Giemsa or MB) and $^1O_2$ probe (DPBF) were 4.62 and 0.076 mM, respectively. The solutions were irradiated with the LED system operating at 625 nm and 3.5 mW cm^{-2} for 210 s. The $^1O_2$ production during irradiation was evaluated by measuring the DPBF absorption every 30 s in a LAMBDA 265 UV/vis spectrophotometer (Perkin Elmer, Boston, MA, USA).

The $\varnothing_\Delta$ was calculated by Eq. (1), where k and k^{std} are the degradation kinetic constants of DPBF under 625 nm illumination for the Giemsa and MB standard obtained from the 415 nm absorbance as a

function of time.

$$\varnothing_{\Delta} = \varnothing_{\Delta}^{std} \cdot \frac{k}{k^{std}} \cdot \frac{I^{sts}}{I} \quad (1)$$

$\varnothing_{\Delta}^{std}$ stands for the quantum yield of the MB standard (0.52) [33,34]. $I^{std}I^{-1} = (1 - 10^{-A_{std}})(1 - 10^{-A})^{-1}$ is the absorption ratio of the photosensitizer (Giemsa) and the standard (MB), in which A and A^{std} are the absorbances at the irradiated wavelength, respectively [31,35].

2.3.2. Reactive Oxygen Species (ROS) generation

ROS production under illumination was assessed according to previous reports with modifications [7,36]. 2.0 mL of the Giemsa photosensitizer at 30 μM and 4 μL of the DHE probe solution at 5 mM were added to a four-sided polished quartz cuvette (10 mm optical path) in DMSO, resulting in a final solution with DHE at 10 μM. This solution was irradiated at 625 nm with 3.5 mW cm^{-2}, and the fluorescence spectra were collected every 120 s for 30 min using a bench-spectrofluorometer (FS-2 FluoroMate, Scinco©, Korea). Excitation was performed at 430 nm, and ROS formation was evaluated by increasing emission in the 440–750 nm region. The ROS production was monitored based on the kinetics of the fluorescent products formed by the interaction between DHE and ROS [36], assuming the rates of generation of fluorescent products and ROS are directly proportional for the Giemsa under red light irradiation [7].

2.3.3. Determination of the $\log P_{O/W}$

The $\log P_{O/W}$ was calculated by the Shake-flask method [37]. The partition coefficients were obtained in a two-phase n-butanol/water ($\log P_{B/W}$) system and correlated with the corresponding values in the n-octanol/water system [37,38]. The measurements were performed using equal volumes of distilled water and n-butanol in a flask and stirred for 24 h at 25 °C. Giemsa was added to the mixture by vortexing vigorously for 3 min and left in the dark to separate the two phases. The absorbance at 528 nm of each phase was measured in a LAMBDA 265 UV/vis spectrophotometer (Perkin Elmer, Boston, MA, USA) to determine the concentration of Giemsa and the partition coefficient [37–39]. Details are reported in section S1 in the supplementary materials.

3. Results and discussion

Fig. 1 shows representative images of *S. aureus* (MSSA and MRSA) colonies on plate count agar for the tested Giemsa concentrations when kept in the dark (non-irradiated) and subjected to 625 nm illumination with an energy dose of 30 J cm^{-2}.

Fig. 2 presents the mean values of the CFU mL^{-1} determined from replicate measurements. The results demonstrate that Giemsa can be successfully applied as PS to photoinactivate MSSA and MRSA strains. No CFUs were observed for antibiotic-susceptible (MSSA) and antibiotic-resistant (MRSA) strains subjected to Giemsa concentration of 10 μM or higher and illumination with a light dose of 30 J cm^{-2}. In turn, the response of the strains to the aPDI was different using sublethal concentrations of PS. For instance, the CFU mL^{-1} decrease of 85 % was observed in MSSA when submitted to Giemsa at 5 μM, while a reduction of 38 % in CFU mL^{-1} was determined to the MRSA strain. Therefore, the antibiotic-susceptible strain is more susceptible to the aPDI using Giemsa than the antibiotic-resistant (MRSA) strain. Antibiotic-sensitive strains are generally more susceptible to aPDI than their multidrug-resistant counterparts [7,27,32,40]. Grinholc et al. (2014) investigated over 400 clinical samples of MRSA and MSSA to conclude that the MRSA strains exhibit less responsiveness to aPDI than MSSA [27]. According to Maish (2015), multidrug-resistant bacteria have higher intrinsic resistance to oxidative stress generated in their environment [41].

Kashef et al. (2012) successfully tested two phenothiazine PSs – MB, and toluidine blue (TBO) – against MSSA and MRSA [40]. A bacterial reduction of 3.1 log and 4.2 log were observed for MRSA and MSSA using TBO at 50 μg mL^{-1} with a light dose of 46.8 J cm^{-2}, respectively.

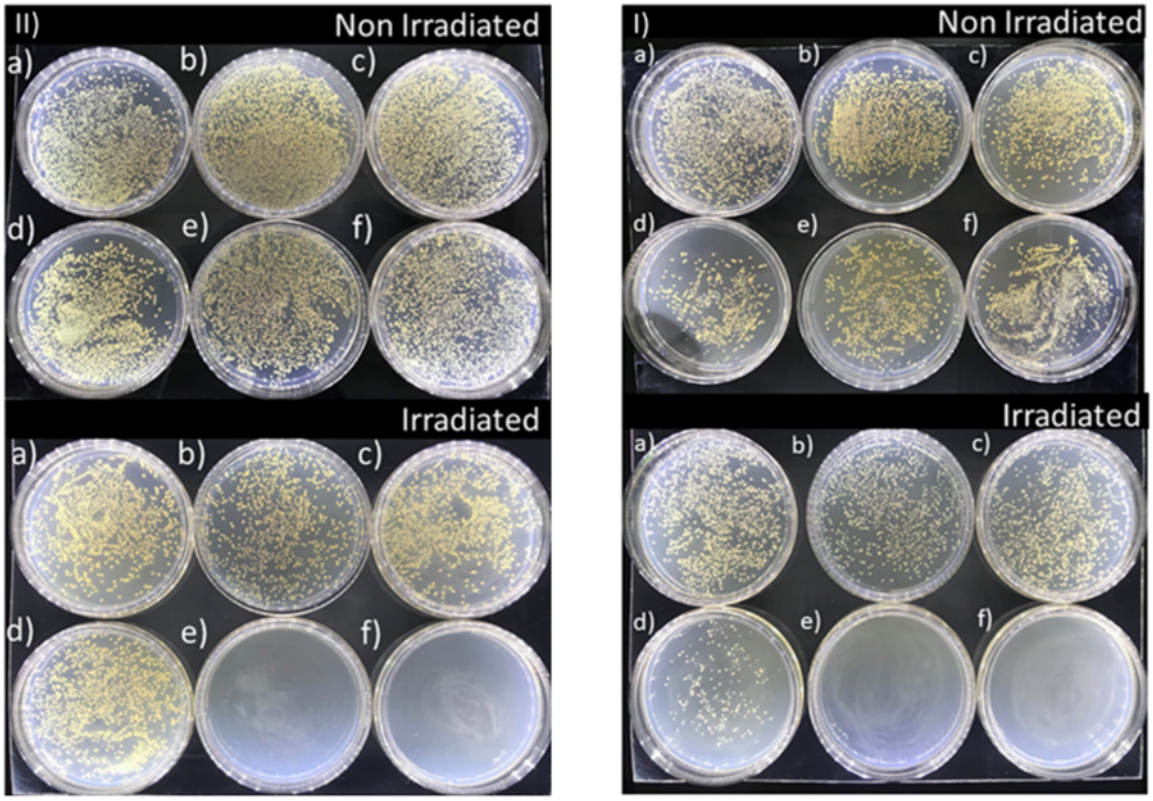

Fig. 1. Growth of (I) MSSA (ATCC 25923) and (II) MRSA (Genbank accession number Mh087437) colonies in Petri dishes containing (a) 0.0, (b) 1.0, (c) 2.5, (d) 5.0, (e) 10.0, and (f) 20.0 μM of Giemsa. The bacterial suspension was illuminated at 625 nm with an energy dose of 0 (non-irradiated) and 30 J cm^{-2} (irradiated).

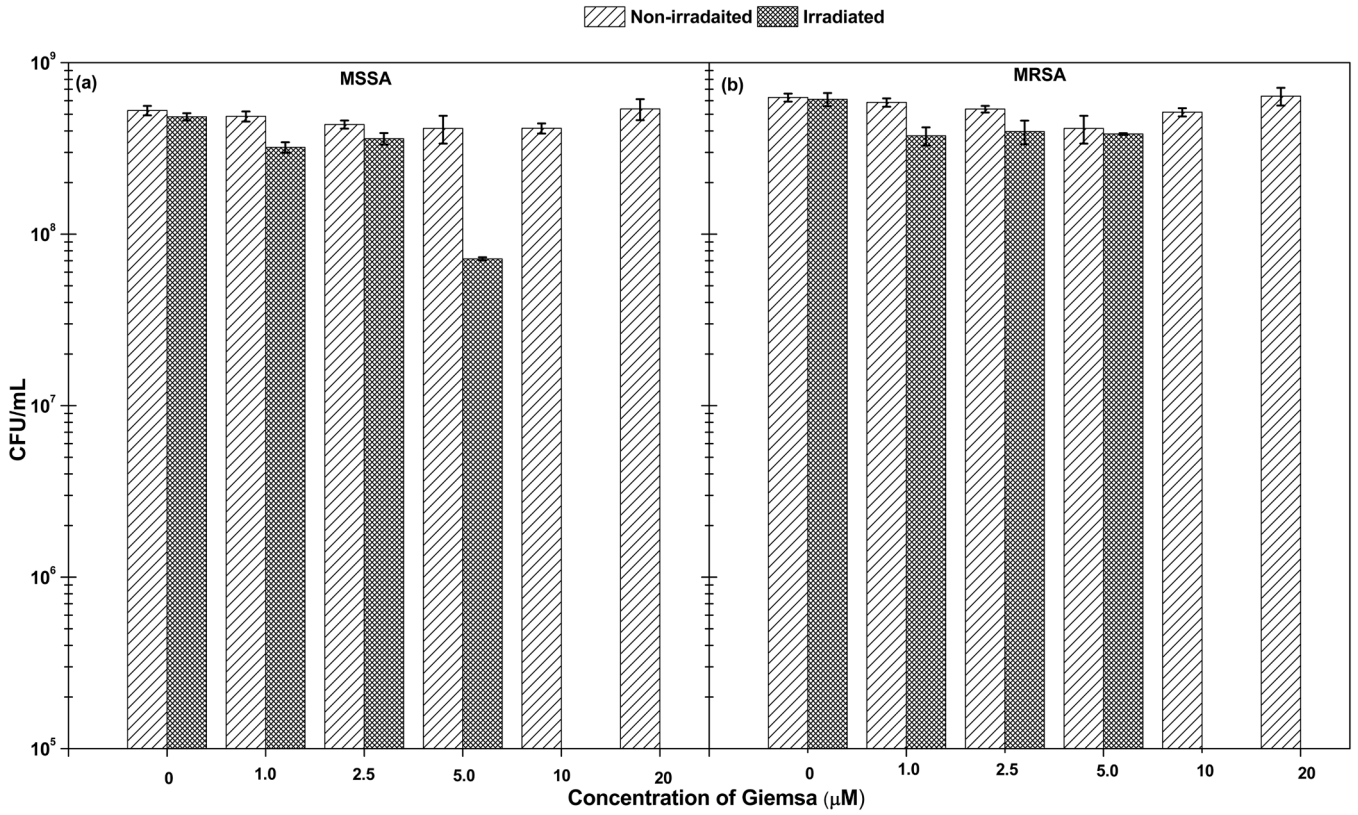

Fig. 2. Mean values of the CFU mL^{-1} of (a) MSSA and (b) MRSA submitted to different Giemsa concentrations. The irradiated group was illuminated at 625 nm with an energy dose of 30 J cm^{-2}. The standard error of the mean is also shown.

Besides, the use of MB at 50 μg mL^{-1} under a light dose of 163.8 J cm^{-2} induced a 2.2 log reduction for MRSA and 3 log for MSSA. [40]. However, the photoinactivation of these strains demanded higher light doses and PS concentrations than those used in the work.

The SEM data confirmed the spherical shapes of *S. aureus* with an approximate diameter of 1 μm and grouped irregularly (Fig. 3). The images also show that the aPDI induced by the Giemsa disrupted the cell membranes of MSSA (Fig. 3b). These damages can lyse the bacteria and deactivate their growth. Differently, no cell damage was promoted by Giemsa on bacteria kept in the dark (Fig. 3a). Similar bacterial damage was observed for MSSA and MRSA submitted to Giemsa and red-light illumination (data not shown).

The ability of a molecule to interact with biological membranes is closely related to its partition coefficient, so the octanol/water partition coefficient is a valuable indicator of the hydrophobicity of a PS and its potential to interact with biological membranes [28]. The higher the partition coefficient, the higher the membrane affinity and hydrophobicity of the PS, facilitating its permeation across lipid-based barriers. The partition coefficient measurements of Giemsa indicate its higher affinity to the octanol phase than the water phase, with $\log P_{O/W} = +0.77$ (Fig. S1 in the supplementary materials). This characteristic makes it a desirable PS as it enhances its interaction with biological membranes.

In aPDI, PS under illumination generates $^1O_2$ and/or ROS, such as superoxide ($O_2^{\bullet}$), hydrogen peroxide (H_2O_2), and hydroxyl ($OH^{\bullet}$), by interacting with the molecular oxygen and promoting cell damage. DPBF and DHE probes were used to determine whether $^1O_2$ and ROS could play a role in the aPDI mediated by Giemsa. Data show that DPBF degraded in the presence of Giemsa as a function of irradiation time at

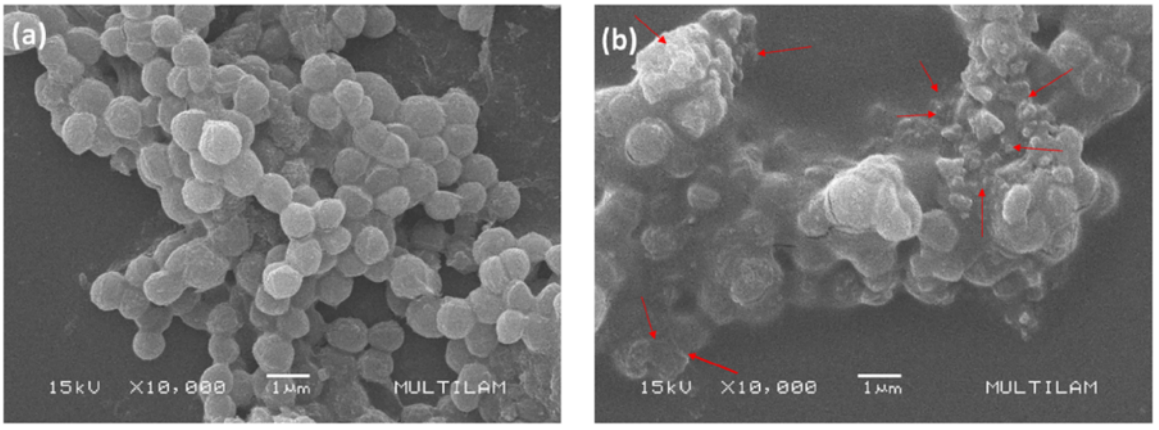

Fig. 3. Representative SEM image of *S. aureus* (MSSA) subjected to Giemsa at 20 μM: (a) strains storage in the dark; and (b) after 625-nm illumination with a light dose of 30 J cm^{-2}. Red arrows indicate cell wall parts partially or entirely damaged.

625 nm (Fig. S2 in the supplementary materials), confirming the $^1O_2$ production in the solution by Giemsa under red-light irradiation. The DPBF degradation occurs due to its reaction with the $^1O_2$ available in the solution, forming an endoperoxide that decomposes into the non-light absorbing molecule, 1,2-dibenzoylbenzene (DBB) [42,43]. The decomposition scheme is depicted in Fig. S3 of the supplementary materials.

The quantum yield of $^1O_2$ production ($\varnothing_\Delta$) for Giemsa was calculated using Eq. (1). The absorbance data at 415 nm of DPBF from Fig. 4 was used along with the $\varnothing_\Delta^{std} = 0.52$ and $k^{std} = (16.3 \pm 0.4)\ 10^{-3}\ s^{-1}$ for the standard PS (MB). Details are reported in section S2 in the supplementary material). The degradation kinetic constant of DPBF (k) was determined from the red fitted curve in Fig. 4b. The obtained value of $\varnothing_\Delta = 0.28$ (Table 1) indicates the Giemsa efficiently produce $^1O_2$ through a type II reaction mechanism (energy transfer) for the targeted inactivation of pathogens [31,43,44].

Additionally, to generate $^1O_2$, Giemsa produced ROS under red-light illumination, as confirmed by the formation of the fluorescent product (2-hydroxyethidium). Fig. 5 shows the fluorescence increase over time during irradiation, and the corresponding spectra are provided in Fig. S4 in the supplementary materials. The formation of 2-hydroxyethidium arises from the degradation of DHE following its interaction with the ROS produced during irradiation. To estimate the ROS production, it was assumed that the fluorescence intensity (I_f) of the generated molecules is directly proportional to the ROS amount ([*ROS*]) produced by the Giemsa under illumination [32]. Accordingly, the ROS production rate equation $-\frac{d[ROS]}{dt} = k_{ROS}\,[DHE][ROS]$ can be rewritten as $\frac{dI_f}{dt} = k_{ROS}\,[DHE]\,I_f$, where k_{ROS} is the apparent rate constant of ROS production. By setting $k_{ROS}\,[DHE] = k_f$ leads to $\frac{dI_f}{dt} = k_f\,I_f$ and, subsequently, $I_f = a(1 - e^{-k_f\,t})$. The fluorescence data shown in Fig. 5 was fitted taking the latter equation yielding $k_f = (1.23 \pm 0.06)10^{-3}\ s^{-1}$. Finally, knowing the k_f and [*DHE*] 10 μM, the apparent rate constant of ROS production of Giemsa was calculated, obtaining a $k_{ROS} = (123 \pm 6)M^{-1}s^{-1}$ (Table 1).

These findings underscore Giemsa's ability to not only produce singlet oxygen ($^1O_2$) but also generate ROS, making it a promising candidate for potential applications in photodynamic therapy, where both $^1O_2$ and ROS play crucial roles in the targeted inactivation of microorganisms.

Table 1
Singlet oxygen quantum yield ($\varnothing_\Delta$) and apparent rate constant of ROS production (k_{ROS}) of Giemsa in DMSO when subjected to illumination at 625 nm with 3.5 mW cm^{-2}.

Probe	Parameter	Value
DPBF	$\varnothing_\Delta$	0.28
DHE	$k_{ROS}(M^{(-1)}s^{(-1)})$	123

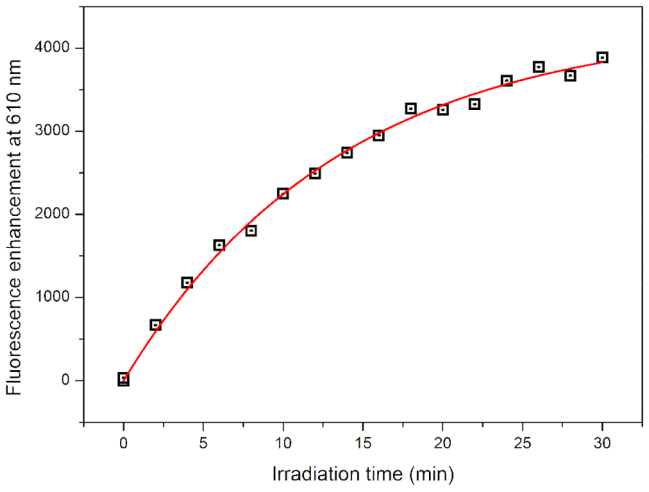

Fig. 5. Fluorescence enhancement at 610 nm of the generated fluorescent product over the illumination time due to the degradation of DHE when interacting with the produced ROS by Giemsa under red-light irradiation at 30 J cm^{-2}. The red line represents the fitting curve ($R^2 = 0.9963$) using $I_f = a(1 - e^{-k_f\,t})$.

4. Conclusion

The Giemsa stain, a common dye used as a biological stain in microscopy analysis, is an efficient PS for targeting methicillin-resistant *Staphylococcus aureus* through photoinactivation without inducing

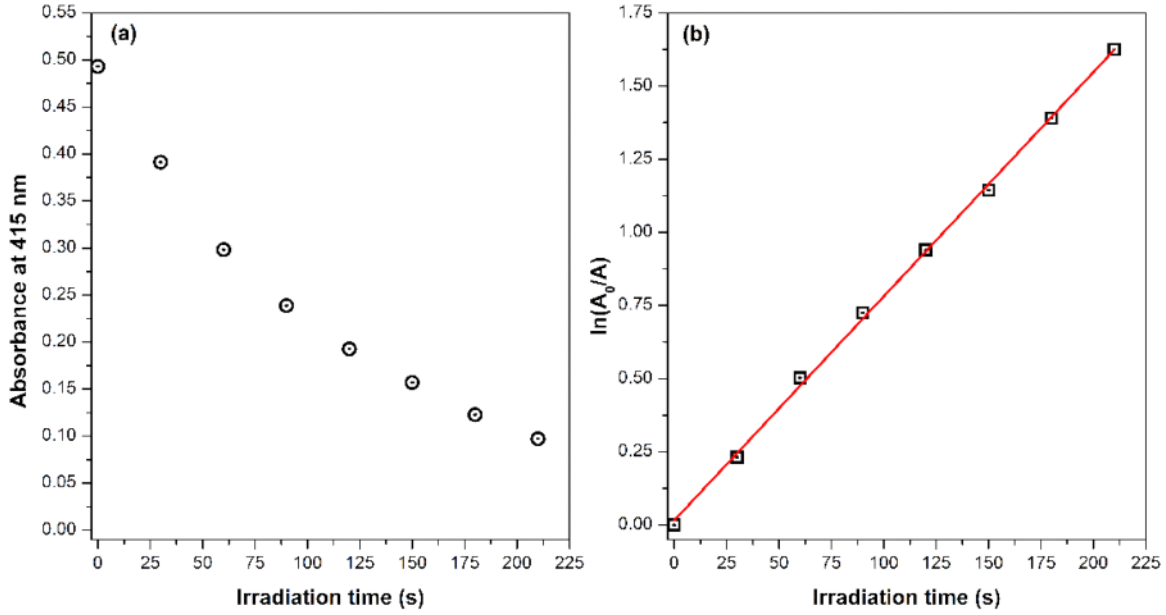

Fig. 4. (a) Absorbance at 415 nm of DPBF in DMSO in the presence of Giemsa (4.62 μM) as a function of irradiation time at 625 nm (3.5 mW); (b) $\ln(A_0\ /A)$ as a function of irradiation time, where A_0 and A are the time-zero absorption and the absorption at 415 nm, respectively. The red line represents the fitted curve used to determine the degradation kinetic constant of DPBF (k).

toxicity in the absence of light. The results support the involvement of both type I and type II photodynamic reaction mechanisms in the antimicrobial photoinactivation process. The ROS production via charge transfer and the $^1O_2$ generation through energy transfer play essential roles in efficiently inactivating bacterial cells. Furthermore, Giemsa's strong membrane affinity underscores its suitability as a PS for antimicrobial photodynamic inactivation. This membrane affinity is a crucial characteristic for an effective PS, as it enhances the photosensitizer's ability to target and interact with biological membranes, ultimately leading to the selective photoinactivation of microbial pathogens. Overall, the findings open new avenues for research and development in the fight against drug-resistant bacterial infections using Giemsa as a photosensitizer in aPDI.

CRediT authorship contribution statement

Cynthia S.A. Caires: Writing – original draft, Methodology, Formal analysis. **Alessandra R. Lima:** Writing – review & editing, Methodology, Formal analysis. **Thalita H.N. Lima:** Writing – review & editing, Methodology. **Cicera M. Silva:** Methodology. **Leandro O. Araujo:** Methodology. **Laís F. Aguilera:** Methodology. **Valter A. Nascimento:** Supervision, Formal analysis, Conceptualization. **Anderson R.L. Caires:** Supervision, Funding acquisition, Formal analysis, Conceptualization, Writing – review & editing. **Samuel L. Oliveira:** Supervision, Funding acquisition, Formal analysis, Conceptualization, Writing – review & editing.

Declaration of competing interest

None.

Acknowledgments

This research was financed by Brazilian funding agencies CNPq (421805/2022-6, 310016/2021-5, 310585/2020-1, and 308232/2021-6), CAPES (88881.311921/2018-01, 88887.311920/2018-00, 88887.311798/2018-00 and 88881.311799/2018-01), and FUNDECT (71/010.797/2022, and 83/013.249/2023). The authors also acknowledge the financial support provided by the National System of Photonics Laboratories-Sisfóton/MCTI (440214/2021-1). This study was supported by the Universidade Federal de Mato Grosso do Sul - UFMS/MEC - Brasil and financed in part by the Coordenação de Aperfeiçoamento de Pessoal de Nível Superior—Brasil (CAPES) - Finance Code 001.

Supplementary materials

Supplementary material associated with this article can be found, in the online version, at doi:10.1016/j.pdpdt.2023.103952.

References

[1] M. Wainwright, Dyes in the development of drugs and pharmaceuticals, Dye. Pigment. 76 (2008) 582–589, https://doi.org/10.1016/j.dyepig.2007.01.015.
[2] B. Fleischer, Editorial: 100 years ago: Giemsa's solution for staining of plasmodia, Trop. Med. Int. Heal. 9 (2004) 755–756, https://doi.org/10.1111/j.1365-3156.2004.01278.x.
[3] E. GURR, Role of eosin in romanowsky staining of malaria nucleus, Nature 202 (1964) 1022–1023, https://doi.org/10.1038/2021022a0.
[4] J.J. Barcia, The Giemsa stain: its history and applications, Int. J. Surg. Pathol. 15 (2007) 292–296, https://doi.org/10.1177/1066896907302239.
[5] B. Fleischer, 100 years ago: Giemsa's solution for staining of plasmodia, Trop. Med. Int. Heal. 9 (2004) 555.
[6] C.S.A. Caires, C.R.B. Leal, C.A.N. Ramos, D. Bogo, A.R. Lima, E.J. Arruda, S. L. Oliveira, A.R.L. Caires, V.A. Nascimento, Photoinactivation effect of eosin methylene blue and chlorophyllin sodium-copper against Staphylococcus aureus and Escherichia coli, Lasers Med. Sci. 32 (2017) 1081–1088, https://doi.org/10.1007/s10103-017-2210-1.
[7] C.S.A. Caires, C.R.B. Leal, A.C.S. Rodrigues, A.R. Lima, C.M. Silva, C.A.N. Ramos, M.R. Chang, E.J. Arruda, S.L. Oliveira, V.A. Nascimento, A.R.L. Caires, Photoinactivation of mcr-1 positive Escherichia coli, Laser Phys. Lett. 15 (2018) 015601, https://doi.org/10.1088/1612-202X/aa86e0.
[8] A.R. Lima, C.M. Silva, C.S.A. Caires, E.D. Prado, L.R.P. Rocha, I. Cabrini, E. J. Arruda, S.L. Oliveira, A.R.L. Caires, Evaluation of eosin-methylene blue as a photosensitizer for larval control of aedes aegypti by a photodynamic process, Insects 9 (2018), https://doi.org/10.3390/insects9030109.
[9] S. A.H., K. J., Methicillin-resistant Staphylococcus aureus, StatPearls [Internet]. Treasure Isl. StatPearls Publ. 2023 Jan-. (n.d.). https://www.ncbi.nlm.nih.gov/books/NBK482221/(accessed September 4, 2023).
[10] J.F. Gibson, J.R. Pidwill, O.T. Carnell et al., Commensal bacteria augment Staphylococcus aureus infection by inactivation of phagocyte- derived reactive oxygen species, (2021) 1–25. 10.1371/journal.ppat.1009880.
[11] R.W. Loftus, F. Dexter, A.D.M. Robinson, K. Words, American journal of infection control methicillin-resistant Staphylococcus aureus has greater risk of transmission in the operating room than methicillin-sensitive S aureus, AJIC Am. J. Infect. Control. 46 (2018) 520–525, https://doi.org/10.1016/j.ajic.2017.11.002.
[12] Global antimicrobial resistance and use surveillance system (GLASS) report 2021, 2021.
[13] S. Lakhundi, K. Zhang, Methicillin-resistant Staphylococcus aureus: molecular characterization, evolution, and epidemiology, Clin. Microbiol. Rev. 31 (2018), https://doi.org/10.1128/CMR.00020-18.
[14] S. Sengupta, M.K. Chattopadhyay, H. Grossart, The multifaceted roles of antibiotics and antibiotic resistance in nature, 4 (2013) 1–13. 10.3389/fmicb.2013.00047.
[15] E. Christaki, M. Marcou, A. Tofarides, Antimicrobial resistance in bacteria: mechanisms, evolution, and persistence, J. Mol. Evol. 88 (2020) 26–40, https://doi.org/10.1007/s00239-019-09914-3.
[16] World Health Organization (WHO), Antimicrobial resistance, (2018). https://www.who.int/en/news-room/fact-sheets/detail/antimicrobial-resistance.
[17] R. Köck, K. Becker, B. Cookson, J.E. van Gemert-Pijnen, S. Harbarth, J. Kluytmans, M. Mielke, G. Peters, R.L. Skov, M.J. Struelens, E. Tacconelli, W. Witte, A. W. Friedrich, Systematic literature analysis and review of targeted preventive measures to limit healthcare-associated infections by meticillin-resistant Staphylococcus aureus, Eurosurveillance 19 (2014), https://doi.org/10.2807/1560-7917.ES2014.19.29.20860.
[18] Antibiotic Resistance Threats in the United States, 2019, Atlanta, Georgia, 2019. 10.15620/cdc:82532.
[19] A. Kourtis, K. Hatfield, J. Baggs, Y. Mu, I. See, E. Epson, J. Nadle, M. Kainer, G. Dumyati, S. Petit, S. Ray, D. Ham, C. Capers, H. Ewing, N. Coffin, L. Mcdonald, J. Jernigan, D. Cardo, Morbidity and mortality weekly report vital signs: epidemiology and recent trends in methicillin-resistant and in methicillin-susceptible *Staphylococcus aureus* bloodstream infections - United States, Morb. Mortal. Wkly. Rep. 68 (2019) 214–219.
[20] G.Y.C. Cheung, J.S. Bae, M. Otto, Pathogenicity and virulence of Staphylococcus aureus, Virulence. 12 (2021) 547–569. 10.1080/21505594.2021.1878688.
[21] United Nations General Assembly, Follow-up to the political declaration of the high-level meeting of the general assembly on antimicrobial resistance, Gen. Assem. Seventy-third Sess. 07777 (2019) 25.
[22] A. Gray, C. Han, C. Bisignano, P. Rao, E. Wool, S.C. Johnson, A.J. Browne, M.G. Chipeta, F. Fell, S. Hackett, G. Haines-Woodhouse, B.H. Kashef Hamadani, E.A.P. Kumaran, B. McManigal, R. Agarwal, S. Akech, S. Albertson, J. Amuasi, J. Andrews, A. Aravkin, E. Ashley, F. Bailey, S. Baker, B. Basnyat, A. Bekker, R. Bender, A. Bethou, J. Bielicki, S. Boonkasidecha, J. Bukosia, C. Carvalheiro, C. Castañeda-Orjuela, V. Chansamouth, S. Chaurasia, S. Chiurchiù, F. Chowdhury, A. J. Cook, B. Cooper, T.R. Cressey, E. Criollo-Mora, M. Cunningham, S. Darboe, N.P. J. Day, M. De Luca, K. Dokova, A. Dramowski, S.J. Dunachie, T. Eckmanns, D. Eibach, A. Emami, N. Feasey, N. Fisher-Pearson, K. Forrest, D. Garrett, P. Gastmeier, A.Z. Giref, R.C. Greer, V. Gupta, S. Haller, A. Haselbeck, S.I. Hay, M. Holm, S. Hopkins, K.C. Iregbu, J. Jacobs, D. Jarovsky, F. Javanmardi, M. Khorana, N. Kissoon, E. Kobeissi, T. Kostyanev, F. Krapp, R. Krumkamp, A. Kumar, H.H. Kyu, C. Lim, D. Limmathurotsakul, M.J. Loftus, M. Lunn, J. Ma, N. Mturi, T. Munera-Huertas, P. Musicha, M.M. Mussi-Pinhata, T. Nakamura, R. Nanavati, S. Nangia, P. Newton, C. Ngoun, A. Novotney, D. Nwakanma, C.W. Obiero, A. Olivas-Martinez, P. Olliaro, E. Ooko, E. Ortiz-Brizuela, A.Y. Peleg, C. Perrone, N. Plakkal, A. Ponce-de-Leon, M. Raad, T. Ramdin, A. Riddell, T. Roberts, J.V. Robotham, A. Roca, K.E. Rudd, N. Russell, J. Schnall, J.A.G. Scott, M. Shivamallappa, J. Sifuentes-Osornio, N. Steenkeste, A.J. Stewardson, T. Stoeva, N. Tasak, A. Thaiprakong, G. Thwaites, C. Turner, P. Turner, H.R. van Doorn, S. Velaphi, A. Vongpradith, H. Vu, T. Walsh, S. Waner, T. Wangrangsimakul, T. Wozniak, P. Zheng, B. Sartorius, A.D. Lopez, A. Stergachis, C. Moore, C. Dolecek C.J. Murray, K.S. Ikuta, F. Sharara, L. Swetschinski, G. Robles Aguilar, M. Naghavi, Global burden of bacterial antimicrobial resistance in 2019: a systematic analysis, Lancet 399 (2022) 629–655, https://doi.org/10.1016/S0140-6736(21)02724-0.
[23] O.O. Ikhimiukor, E.E. Odih, P. Donado-Godoy, I.N. Okeke, A bottom-up view of antimicrobial resistance transmission in developing countries, Nat. Microbiol. 7 (2022) 757–765, https://doi.org/10.1038/s41564-022-01124-w.
[24] P. Dadgostar, Antimicrobial resistance: implications and costs, Infect. Drug Resist. 12 (2019) 3903–3910, https://doi.org/10.2147/IDR.S234610.
[25] World Bank, Drug-resistant infections: a threat to our economic future, World Bank Rep. 2 (2017) 1–132.
[26] T. Frieden, Antibiotic resistance threats in the United States, Cent. Dis. Control Prev. (2013). www.cdc.gov/drugresistance/pdf/ar-threats-2013-508.pdf.
[27] M. Grinholc, A. Rapacka-Zdonczyk, B. Rybak, F. Szabados, K.P. Bielawski, Multiresistant strains are as susceptible to photodynamic inactivation as their naïve counterparts: protoporphyrin IX-mediated photoinactivation reveals differences between methicillin-resistant and methicillin-sensitive staphylococcus aureus

strains, Photomed. Laser Surg. 32 (2014) 121–129, https://doi.org/10.1089/pho.2013.3663.
[28] A.P. Castano, T.N. Demidova, M.R. Hamblin, Mechanisms in photodynamic therapy: part one—photosensitizers, photochemistry and cellular localization, Photodiagn. Photodyn. Ther. 1 (2004) 279–293, https://doi.org/10.1016/S1572-1000(05)00007-4.
[29] L. Huang, T. Dai, M.R. Hamblin, Antimicrobial photodynamic inactivation and photodynamic therapy for infections, in: 2010: pp. 155–173. 10.1007/978-1-60761-697-9_12.
[30] J. Chen, W. Wang, P. Hu, D. Wang, F. Lin, J. Xue, Z. Chen, Z. Iqbal, M. Huang, Dual antimicrobial actions on modified fabric leads to inactivation of drug-resistant bacteria, Dye. Pigment. 140 (2017) 236–243, https://doi.org/10.1016/j.dyepig.2017.01.032.
[31] R.C. Pivetta, B.L. Auras, B. de Souza, A. Neves, F.S. Nunes, L.H.Z. Cocca, L. De Boni, B.A. Iglesias, Synthesis, photophysical properties and spectroelectrochemical characterization of 10-(4-methyl-bipyridyl)-5,15-(pentafluorophenyl)corrole, J. Photochem. Photobiol. A Chem. 332 (2017) 306–315, https://doi.org/10.1016/j.jphotochem.2016.09.008.
[32] C.S.A. Caires, C.M. Silva, A.R. Lima, L.M. Alves, T.H.N. Lima, A.C.S. Rodrigues, M. R. Chang, S.L. Oliveira, C. Whitby, V.A. Nascimento, A.R.L. Caires, Photodynamic inactivation of methicillin-resistant staphylococcus aureus by a natural food colorant (e-141II), Molecules 25 (2020), https://doi.org/10.3390/molecules25194464.
[33] M. Nemoto, H. Kokubun, M. Koizumi, Determination of the S * –T transition probabilities of some xanthene and thiazine dyes on the basis of the T-energy transfer. I. Experiment in ethanol solutions, Bull. Chem. Soc. Jpn. 42 (1969) 1223–1230, https://doi.org/10.1246/bcsj.42.1223.
[34] R.H. Young, D. Brewer, R.A. Keller, Determination of rate constants of reaction and lifetimes of singlet oxygen in solution by a flash photolysis technique, J. Am. Chem. Soc. 95 (1973) 375–379, https://doi.org/10.1021/ja00783a012.
[35] C. Hadjur, N. Lange, J. Rebstein, P. Monnier, H. Van Den Bergh, G. Wagnières, Spectroscopic studies of photobleaching and photoproduct formation of meta (tetrahydroxyphenyl)chlorin (m-THPC) used in photodynamic therapy. The production of singlet oxygen by m-THPC, J. Photochem. Photobiol. B Biol. 45 (1998) 170–178, https://doi.org/10.1016/S1011-1344(98)00177-8.
[36] C.S.A. Caires, C.M. Silva, A.R. Lima, L.M. Alves, T.H.N. Lima, A.C.S. Rodrigues, M. R. Chang, S.L. Oliveira, C. Whitby, V.A. Nascimento, A.R.L. Caires, Photodynamic inactivation of methicillin-resistant staphylococcus aureus by a natural food colorant (E-141ii), Molecules 25 (2020) 4464.
[37] F. Engelmann, S. Rocha, H. Toma, K. Araki, M. Baptista, Determination of n-octanol/water partition and membrane binding of cationic porphyrins, Int. J. Pharm. 329 (2007) 12–18, https://doi.org/10.1016/j.ijpharm.2006.08.008.
[38] L. Alonso, R.N. Sampaio, T.F.M. Souza, R.C. Silva, N.M.B. Neto, A.O. Ribeiro, A. Alonso, P.J. Gonçalves, Photodynamic evaluation of tetracarboxy-phthalocyanines in model systems, J. Photochem. Photobiol. B Biol. 161 (2016) 100–107, https://doi.org/10.1016/j.jphotobiol.2016.05.008.
[39] A.R. Lima, C.M. da Silva, C.S.A. Caires, H. Chaves, A.S. Pancrácio, E.J. de Arruda, A.R.L. Caires, S.L. Oliveira, Photoinactivation of Aedes aegypti larvae using riboflavin as photosensitizer, Photodiagn. Photodyn. Ther. 39 (2022) 103030, https://doi.org/10.1016/j.pdpdt.2022.103030.
[40] N. Kashef, G.Ravaei Sharif Abadi, G.E. Djavid, Phototoxicity of phenothiazinium dyes against methicillin-resistant Staphylococcus aureus and multi-drug resistant Escherichia coli, Photodiagn. Photodyn. Ther. 9 (2012) 11–15, https://doi.org/10.1016/j.pdpdt.2011.11.004.
[41] T. Maisch, Resistance in antimicrobial photodynamic inactivation of bacteria, Photochem. Photobiol. Sci. 14 (2015) 1518–1526, https://doi.org/10.1039/C5PP00037H.
[42] P. Carloni, E. Damiani, L. Greci, P. Stipa, F. Tanfani, E. Tartaglini, M. Wozniak, On the use of 1,3-diphenylisobenzofuran (DPBF). Reactions with carbon and oxygen centered radicals in model and natural systems, Res. Chem. Intermed. 19 (1993) 395–405, https://doi.org/10.1163/156856793×00181.
[43] X.-F. Zhang, X. Li, The photostability and fluorescence properties of diphenylisobenzofuran, J. Lumin. 131 (2011) 2263–2266, https://doi.org/10.1016/j.jlumin.2011.05.048.
[44] A. Juzeniene, K.P. Nielsen, J. Moan, Biophysical Aspects of Photodynamic Therapy, J. Environ. Pathol. Toxicol. Oncol. 25 (2006) 7–28, https://doi.org/10.1615/JEnvironPatholToxicolOncol.v25.i1-2.20.